



Published in final edited form as:

Laryngoscope. 2010 August ; 120(8): 1619–1624. doi:10.1002/lary.20979.

Flexible cochlear microendoscopy in the gerbil†

Adam P. Campbell, BA, Thomas A. Suberman, BA, Craig A. Buchman, MD, Douglas C. Fitzpatrick, PhD, and Oliver F. Adunka, MD

Department of Otolaryngology/Head and Neck Surgery, University of North Carolina at Chapel Hill, Chapel Hill, North Carolina, U.S.A.

Abstract

Objective—To validate the scientific utility of flexible cochlear microendoscopy in the gerbil. This model is currently being developed to study the effects of intracochlear electrode positioning on functional parameters.

Methods—A flexible fiberoptic microendoscope featuring a light channel and an outer diameter of 0.4 mm was especially modified to allow intracochlear visualization. Specifically, the focus distance was reduced to 1 mm and the optical properties were modified so that visualization was adequate when submerged in perilymphatic fluid. This endoscope was used to view intracochlear contents and monitor the progress of electrode insertions in 11 gerbils. The endoscopic data estimating the site of damage were compared to postmortem microdissections.

Results—The endoscope allowed for adequate visualization of intracochlear content in all animals. The site of electrode contact seen in the endoscope was confirmed in the microdissected cochleae in 10 of 11 cases, indicating the endoscope's ability to correctly identify the site of intracochlear trauma in this animal model.

Conclusions—The current report demonstrates the feasibility of intracochlear microendoscopy in an animal model of hearing preservation cochlear implantation.

INTRODUCTION

Over the past two decades, endoscopic techniques have continued to evolve and are now staples of practically every medical specialty. In sinus surgery, for example, endoscopic procedures have almost entirely replaced both open approaches and microscopic methods. Recent advances in laparoscopic technology have even allowed for endoscopic procedures of the neck such as minimal incision thyroidectomies.

In otology & neurotology, endoscopes have been used in experimental settings, only. Multiple aspects of temporal bone surgery, however, might benefit from this technology due to the small anatomical scale as well as the endoscope's ability to provide an angled view. The inner ear provides an even greater challenge: first, the inner ear hosts the delicate structures of hearing and balance, which are at risk from the mechanical interaction with the electrode carrier. Second, the shape of the cochlear fluid spaces requires a flexible device in order to visualize more distal regions. Furthermore, the maintenance of cochlear function

†This work was supported by MED-EL Corporation. The authors have no other funding, financial relationships, or conflicts of interest to disclose.

*Correspondence: Oliver F. Adunka MD, Otology, Neurotology, Skull Base Surgery, Department of Otolaryngology/Head and Neck Surgery, University of North Carolina at Chapel Hill, POB, 170 Manning Drive, CB# 7070, Chapel Hill, NC 27599-7070 (adunka@med.unc.edu).

requires preservation of labyrinthine fluid dynamics and adequate visualization instruments have to work underwater.

Previously, cochlear endoscopy has been attempted in several studies in both humans and animals. These studies were primarily limited by the low resolution of the devices and the lack of a clinical application^{1,2}. Specifically, cochlear endoscopy was proposed as an adjunct to cochlear implantation in order to identify morphologic changes such as fibrosis or ossification. Thus, functional aspects have not been considered also due to the assumption that trauma to intracochlear structures might bear little or no effect on cochlear implant performance³. Recent data, however, suggests the contrary, in that poor cochlear implant performance has been linked to electrode dislocations and intracochlear trauma^{4,5}. Also, the advent of combined stimulation paradigms such as electric acoustic stimulation (EAS)⁶, hybrid stimulation⁷, or partial deafness cochlear implantation (PDCI)⁸ has demonstrated the importance of atraumatic cochlear implantation with both the morphologic and functional preservation of inner ear structures⁹.

In this article, we would like to revisit intracochlear endoscopy. Specifically, we would like to evaluate its utility in an animal model we developed for hearing preservation during cochlear implantation. In this model, we were able to record electrophysiologic changes as a result of intracochlear electrode insertions. In our first few experiments, we were able to demonstrate the overall feasibility of detecting even minor cochlear damage using an intracochlear electrode to record acoustically evoked potentials¹⁰. To further advance this set of experiments and in an effort to move closer to the clinical scenario, direct visualization of the electrode within the cochlea was needed. Thus, we hoped that cochlear endoscopy would provide a useful tool to detect intracochlear electrode positioning and interaction of the electrode with specific cochlear structures. Also, these findings could help to re-evaluate updated technology of cochlear endoscopy for possible future clinical use. Therefore, the aim of this paper was to establish cochlear microendoscopy as a scientific tool and to determine its utility in predicting intracochlear electrode positioning in the gerbil.

METHODS

The gerbil was chosen for our animal model because it has good low frequency hearing and the bulla provides easy access to the round window as well as to the basal turn. Preliminary functional electrophysiologic data have been reported elsewhere¹⁰ and this report's aim is to validate the endoscope for future studies. All animals were handled and housed according to the standards described by the National Institutes of Health Committee on Care and Use of Laboratory Animals, using protocols approved by the Institutional Animal Care and Use Committee at the study institution.

Animal handling

Surgeries and recordings were performed under deep urethane anesthesia (25% solution in saline, 1.5 g/kg, IP). Once anesthesia was induced, the animal was moved to a double-walled, sound attenuated booth for the remainder of the experiment (up to 10 hours). The body core temperature was monitored with a rectal probe and maintained at approximately 37°C with reusable heating pads. The animal's heart rate was monitored with electrodes placed on the chest and back.

Endoscope

The microendoscope is a flexible fiberoptic, custom-built device that has a 0.4 mm outer diameter (0.3-mm without the channel delivering the light) and is 62-mm long (Zibacorp, Westport, MA). It features 3,000 fibers, has a 1-mm focal length, a 50° field of view (in

saline) and $\sim 50\times$ magnification. It is attached to an adjustable, external light source (Welch Allyn, Skaneateles Falls, NY) and a color, closed circuit television camera (ELMO, Plainview, NY), which subsequently feeds to a computer monitor (Figure 1).

Surgical Procedure

After anesthesia was induced, hair was removed from the postauricular skin and a vertical skin incision was performed. Superficial tissues were dissected and the bone of the bulla was identified. The pinna was removed to allow consistent sound delivery. The bony bulla was opened and the round window niche, the spiral modiolar artery, and all other structures of the bulla were identified. The microendoscope was attached to a mechanical micromanipulator, which allowed for precise placement of the endoscope. The lens of the microendoscope was placed against the intact round window membrane and its angle was manipulated until the basilar membrane, the osseous spiral lamina, and the spiral ligament were adequately visualized.

Since the round window niche was occupied, a cochleostomy was made in the basal turn of the cochlea adjacent to the spiral modiolar artery using either a perforator used for stapes surgery or a flexible CO₂ laserfiber (OmniGuide, Cambridge, MA). This step required extremely careful handling of the cochlea to avoid intracochlear trauma or perilymph loss. The recording electrode used was a 50 μm diameter, Teflon-insulated tungsten-iridium wire. The electrode was rigid and attached to a hydraulic micro-drive, which was controlled from outside the sound booth in steps as small as 1 μm . The electrode was attached to a micromanipulator and placed at the entrance to the cochleostomy. Figure 2 shows the positioning of both the microendoscope (in the round window niche) and electrode (via cochleostomy) during an experiment.

Electrode Advancement

Once the microendoscope and electrode were in proper position, the brightness level was adjusted in order to optimally visualize the intracochlear structures. The electrode was slowly advanced with the hydraulic micro-drive. Using the live endoscopic image for guidance, the electrode was slowly advanced until it approached intracochlear structures. Due to the angle dictated in part by the shape of the bony lateral wall of the basal cochlear turn, the electrode was either aimed at the basilar membrane or the osseous spiral lamina. If multiple penetrations were desired, the endoscope was used to reposition the electrode within the cochlea. As the electrode was advanced, the depths and corresponding images were recorded.

Assessment of Cochlear Status and Electrode Position

After completion of the experiment, each animal was sacrificed and the cochlea was fixed and removed en block. The whole mounts were decalcified and stained with toluidine blue. A microscope with camera attachment was used to analyze and photographically document and determine the site of intracochlear trauma.

Data Analysis

The site of intracochlear impact as visualized by the microendoscope was graded independently by four investigators (OFA, APC, TAS, DCF). The location as determined from the endoscopic images was then compared to the site of impact determined from the microdissections.

RESULTS

Complete datasets (endoscopic data as well as microdissection results) were acquired from 10 animals and 11 penetrations. Each set of endoscopic images was evaluated independently as detailed above. Each investigator determined the likely site of electrode impaction at the deepest insertion depth without knowledge of the correlating microdissection. These results were compared to the damage evaluated via histology, which served as the standard.

The endoscopic image in its position on the round window provided visualization of the basal turn scala tympani. Electrode insertions were performed through an atraumatic cochleostomy and electrophysiologic recordings indicated the non-traumatic nature of the cochleostomy. These data are presented elsewhere. The flexible nature of the microendoscope allowed visualizations using different angles so to that the electrode could be adequately imaged. In each case, the entire electrode penetration starting at the cochleostomy to the site of impact on the OSL and/or BM was visualized using the endoscope.

As shown in Figure 3 (gerbil #8), the basilar membrane appears dark due to its relative transparency and the stria vascularis' pigmented nature, while the spiral ligament, osseous spiral lamina and electrode are more reflective and appear brighter. Figure 3 shows the endoscopic images of two distinct penetrations in the same animal. In the first penetration, the microendoscope was used to observe the advancement of the electrode as it impacted the osseous spiral lamina, as shown in Figure 3B. Following this damage, the electrode was retracted and its angle of insertion was slightly adjusted. The microendoscopic image at the deepest insertion of the second penetration is shown in Figure 3B, with the electrode tip located at the basilar membrane. The corresponding histologic damage is shown in Figure 3C. A deep scrape (non full thickness) in the osseous spiral lamina from penetration #1 and a disruption of the basilar membrane from penetration 2 can be observed.

Figure 4 shows various penetrations illustrating different trauma locations. Typically, a good correlation between the investigator's estimated site of impact and the actual trauma location as seen during the microdissection was observed. In the one case where the endoscopic image did not correlate with the subsequent histology, the image at the deepest insertion point did not clearly show the tip of the electrode. Therefore, it appeared as though the electrode as located in the BM, while the histology showed substantial damage to the OSL.

DISCUSSION

In this paper, we were able to assess the feasibility of cochlear microendoscopy in an animal model of hearing preservation cochlear implantation. Our results indicate that despite this technology's limitations, it provided the investigators with useful information on the intracochlear position of a rigid intracochlear electrode relative to cochlear microanatomy. Therefore, our results might prompt re-evaluation of cochlear endoscopy not just in the animal model but also for human application. Specifically, the advent of new stimulation paradigms such as electric acoustic stimulation^{6-8,11} with the need to provide non-destructive intracochlear electrode placements makes this technology potentially clinically useful.

Recent research, for example, has demonstrated a relationship between the exact intracochlear positioning of individual electrode contacts with postoperative speech perception performance⁴. During this research, the number of electrode contacts in scala vestibuli has been correlated with below average cochlear implant performance scores. Furthermore, electrode dislocations into scala vestibuli have been associated with marked intracochlear trauma¹². Hence, this data suggests that intracochlear trauma can result in

lower speech discrimination scores with the cochlear implant. This research has been supplemented by another dataset essentially suggesting similar findings in a larger cohort of adult cochlear implant recipients⁵.

Therefore, structural preservation of intracochlear contents might not just be critical for hearing preservation purposes, but rather it might be a fundamental aspect of every cochlear implant procedure. Several other developments have helped to minimize intracochlear trauma by employing correct cochleostomy techniques^{13,14} as well as through modified and less traumatic electrode arrays¹⁵. In some instances, however, use of direct visualization might demonstrate beneficial especially if greater resolution capabilities can be integrated in future technology.

Cochlear endoscopy was first attempted in cadaveric human temporal bone studies, in which 0.7-mm and 1.0-mm diameter endoscopes were passed into the scala tympani². In multiple later studies, endoscopes were inserted into the scala tympani of live, human subjects in order to visualize obstructions in the cochlea during cochlear implantation^{1,16,17}. These early endoscope experiments evidenced the ability to visualize intracochlear structures, including the basilar membrane and osseous spiral lamina. Unfortunately, the usefulness of this imaging data was limited by marginal image quality. In addition, the insertion of these larger devices seemed to cause intracochlear trauma² and subsequent hearing loss in animal models³. As endoscopic technology advanced, later studies demonstrated the ability to visualize the basilar membrane and osseous spiral lamina through the round window to observe cochlear blood flow¹⁸. Our study shows that with the latest endoscope technology the technique can also be used to visualize the an implant electrode in relation to cochlear structures.

Optical coherence tomography (OCT) has emerged as another possible answer to real time imaging of the intracochlear structures that may be useful for electrode guidance during implantation. In a study utilizing OCT to visualize the basal turn of the porcine cochlea, very high-resolution images could be obtained. However, the overlying bone must be thinned in order to obtain adequate light penetration¹⁹. High frequency ultrasound has also been tested to visualize the inner ear, but the current devices are too wide to be used in vivo²⁰.

Given these prior results and advances in technology, we returned to the microendoscope to visualize the basal turn of the cochlea. Previous experiments utilized 0.7-mm and 1.0-mm diameter endoscopes containing 1,600 quartz fibers, a 55° FOV, a 1-25 mm depth of focus, and 60 × magnification. We used a smaller, higher resolution microendoscope that is 0.4-mm in diameter including a light channel with 3,000 fibers, a 50° FOV, 1-mm depth of focus, and 50× magnification. This change in size and resolution allowed for increased manipulation within the round window niche, higher resolution images, and decreased risk of intracochlear trauma.

On the downside, the image only allows for a 2-dimensional view and the estimation of electrode positioning was only possible with the endoscope placed very close to the targeted structure. Also, the current approach allowed us to look into the cochlear but not to look from within the basal turn. Therefore, only structures adjacent to the endoscope were visualized by the device's placement on the round window membrane. Lastly, the surgical approach had a substantial learning curve in that early experiments resulted in inadvertent manipulations due to the complicated experimental set-up.

As a research tool, however, intracochlear microendoscopy provided a useful means for evaluating electrode position in the basal turn of the cochlea in this animal model. The clinical utility of cochlear endoscopy in human subjects, though, remains to be determined.

CONCLUSIONS

This study demonstrates the feasibility of using a microendoscope for evaluating electrode positioning relative to cochlear microanatomy within the basal turn of the gerbil. As this imaging modality is noninvasive and nondestructive, it may provide scientists a means for better understanding intracochlear mechanics and trauma secondary to electrode insertion. Our research is ongoing in that we attempt to correlate findings presented herein with functional data represented through electrophysiologic parameters.

REFERENCES

1. Balkany T. Endoscopy of the cochlea during cochlear implantation. *Ann Otol Rhinol Laryngol.* 1990; 99:919–922. [PubMed: 2241019]
2. Balkany T, Fradis M. Flexible fiberoptic endoscopy of the cochlea: human temporal bone studies. *Am J Otol.* 1991; 12:46–48. [PubMed: 2012189]
3. Balkany T, Hodges AV, Whitehead M, Memari F, Martin GK. Cochlear endoscopy with preservation of hearing in guinea pigs. *Otolaryngol Head Neck Surg.* 1994; 111:439–445. [PubMed: 7936675]
4. Skinner MW, Holden TA, Whiting BR, et al. In vivo estimates of the position of advanced bionics electrode arrays in the human cochlea. *Ann Otol Rhinol Laryngol Suppl.* 2007; 197:2–24. [PubMed: 17542465]
5. Aschendorff A, Kromeier J, Klenzner T, Laszig R. Quality control after insertion of the nucleus contour and contour advance electrode in adults. *Ear Hear.* 2007; 28:75S–79S. [PubMed: 17496653]
6. Gstoettner WK, van de Heyning P, O'Connor AF, et al. Electric acoustic stimulation of the auditory system: results of a multi-centre investigation. *Acta Otolaryngol.* 2008; 128:968–975. [PubMed: 19086194]
7. Gantz BJ, Hansen MR, Turner CW, Oleson JJ, Reiss LA, Parkinson AJ. Hybrid 10 clinical trial: preliminary results. *Audiol Neurootol.* 2009; 14(Suppl 1):32–38. [PubMed: 19390173]
8. Skarzynski H, Lorens A, Piotrowska A. A new method of partial deafness treatment. *Med Sci Monit.* 2003; 9:CS20–24. [PubMed: 12709676]
9. Adunka O, Gstoettner W, Hambek M, Unkelbach MH, Radeloff A, Kiefer J. Preservation of basal inner ear structures in cochlear implantation. *ORL J Otorhinolaryngol Relat Spec.* 2004; 66:306–312. [PubMed: 15668529]
10. Adunka, OF.; Mlot, S.; Suberman, TA., et al. Intracochlear recordings of electrophysiologic parameters indicating cochlear damage. submitted
11. Fraysse, B.; K., A.; R., B., et al. Conservation of residual hearing and electro-acoustic stimulation in recipients of the Nucleus 24 Contour Advance cochlear implant. VIII International Cochlear Implant Conference; Indianapolis, IN. 2004. p. 126
12. Adunka O, Kiefer J, Unkelbach MH, Radeloff A, Gstoettner W. Evaluating cochlear implant trauma to the scala vestibuli. *Clin Otolaryngol.* 2005; 30:121–127. [PubMed: 15839863]
13. Adunka OF, Radeloff A, Gstoettner WK, Pillsbury HC, Buchman CA. Scala tympani cochleostomy II: topography and histology. *Laryngoscope.* 2007; 117:2195–2200. [PubMed: 17909447]
14. Briggs RJ, Tykocinski M, Stidham K, Roberson JB. Cochleostomy site: implications for electrode placement and hearing preservation. *Acta Otolaryngol.* 2005; 125:870–876. [PubMed: 16158535]
15. Adunka O, Kiefer J, Unkelbach MH, Lehnert T, Gstoettner W. Development and evaluation of an improved cochlear implant electrode design for electric acoustic stimulation. *Laryngoscope.* 2004; 114:1237–1241. [PubMed: 15235353]
16. Baumgartner WD, Franz P, Gstoettner W, Hamzavi J. Cochlea endoscopy in vivo. *Adv Otorhinolaryngol.* 1997; 52:62–65. [PubMed: 9042452]
17. Kautzky M, Susani M, Franz P, Zrunek M. Flexible fiberoptic endoscopy and laser surgery in obliterated cochleas: human temporal bone studies. *Lasers Surg Med.* 1996; 18:271–277. [PubMed: 8778523]

18. Monfared A, Blevins NH, Cheung EL, Jung JC, Popelka G, Schnitzer MJ. In vivo imaging of mammalian cochlear blood flow using fluorescence microendoscopy. *Otol Neurotol*. 2006; 27:144–152. [PubMed: 16436982]
19. Sepehr A, Djalilian HR, Chang JE, Chen Z, Wong BJ. Optical coherence tomography of the cochlea in the porcine model. *Laryngoscope*. 2008; 118:1449–1451. [PubMed: 18496151]
20. Brown JA, Torbatian Z, Adamson RB, et al. High-frequency ex vivo ultrasound imaging of the auditory system. *Ultrasound Med Biol*. 2009; 35:1899–1907. [PubMed: 19679390]



Figure 1. Flexible fiberoptic microendoscope (Zibracorp, Westport, MA): 0.3 mm outer diameter, visualization channel only, 0.4 mm outer diameter including light channel). Length: 62 mm, focal length: 1 mm, 50° FOV, ~50 × magnification; shown attached to color CCD TV Camera (ELMO, Plainview, NY, USA). The small inlet shows the tip of the endoscope next to a millimeter scale.

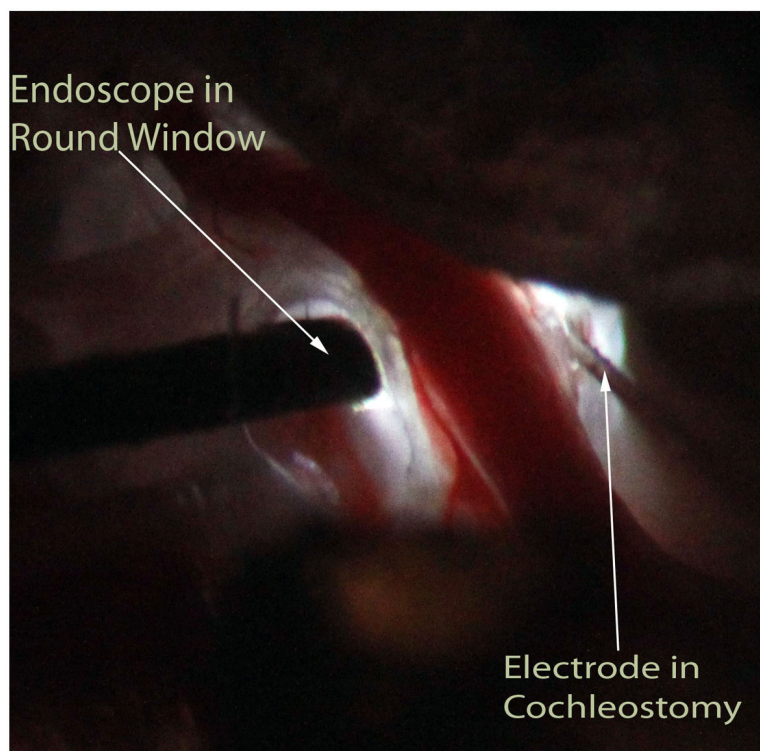
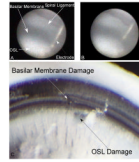


Figure 2. Right ear of gerbil after posterior exposure of bulla with view of the basal cochlear turns. The light is provided via the endoscope. The endoscope has been placed onto the intact round window membrane while the rigid electrode was inserted through a cochleostomy made in the scala tympani of the basal turn of the cochlea.

**Figure 3.**

Gerbil #8, Penetrations 1 and 2: **A:** Intracochlear structures identified through the microendoscope (right ear) when placed within the round window niche. First penetration. The basilar membrane appears dark due to its transparency to light. The spiral ligament, osseous spiral lamina (OSL) and electrode all appear bright. This image represents the deepest insertion of the electrode in this penetration, where the electrode impacts the OSL. **B:** Second electrode penetration in the same case. The image is at the deepest penetration depth with the electrode impacting the basilar membrane. **C:** Corresponding microdissection image indicating distinct damage on the basilar membrane and osseous spiral lamina for the two penetrations.

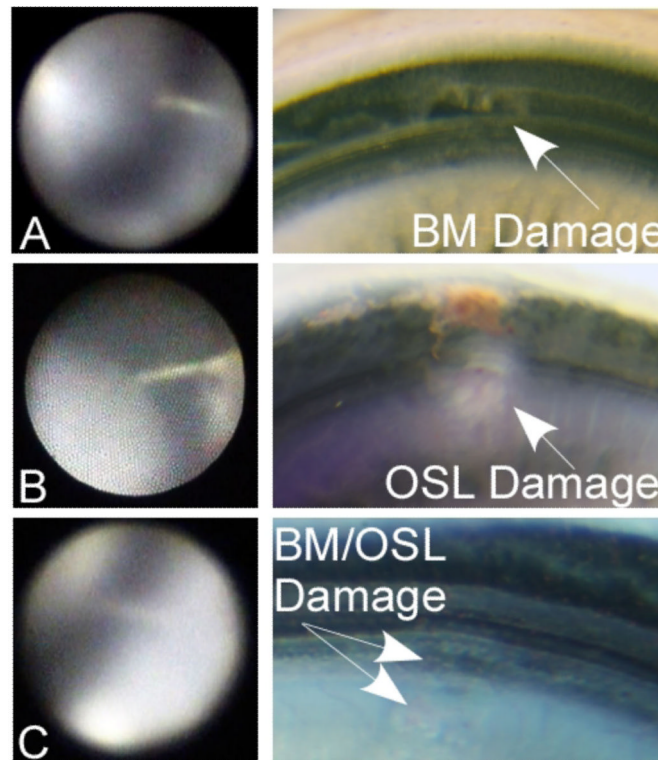


Figure 4.

Representative cases with endoscopic images and correlating microdissections: Case #7; **A**: Electrode tip directed towards/touching the basilar membrane (BM). The corresponding microdissection demonstrates full thickness damage to the basilar membrane. Case #2; **B**: Electrode seems directed towards the osseous spiral lamina (OSL). Corresponding histology confirms full thickness injury to the OSL. Case #4; **C**: Endoscopic image suggesting electrode trauma to the OSL or the junction of the OSL and the BM. Corresponding microdissection shows superficial trauma to the OSL/BM.

Table 1

Data on all 10 animals and 11 electrode penetrations.

| Gerbil # | Endoscope | | | | Damage | |
|----------|-----------|--------|--------|--------|--------|----------------|
| | Histology | #1 | #2 | #3 | | #4 |
| 1 | BM | BM | BM | BM/OSL | BM | full thickness |
| 2 | OSL | OSL | OSL | OSL | OSL | full thickness |
| 3 | OSL | BM | BM | BM | BM | superficial |
| 4 | BM/OSL | OSL | BM/OSL | OSL | BM/OSL | superficial |
| 5 | BM/OSL | BM/OSL | BM | BM | BM | full thickness |
| 6 | BM/OSL | BM | BM | BM/OSL | BM | superficial |
| 7 | BM | BM | BM | OSL | BM/OSL | full thickness |
| | OSL | OSL | BM/OSL | OSL | OSL | superficial |
| 8 | | | | | | |
| 9 | OSL | OSL | OSL | OSL | OSL | full thickness |
| 10 | OSL | BM | OSL | BM/OSL | BM | superficial |

Endoscopic data evaluated independently by 4 investigators (#1-4)

Gerbil #8 had two distinct electrode penetrations